A classification scheme for chimera states

Cite as: Chaos **26**, 094815 (2016); https://doi.org/10.1063/1.4959804
Submitted: 29 February 2016 . Accepted: 13 July 2016 . Published Online: 02 August 2016

Felix P. Kemeth, Sindre W. Haugland, Lennart Schmidt, Ioannis G. Kevrekidis, and Katharina Krischer

A classification scheme for chimera states

Felix P. Kemeth,[1,2,3] Sindre W. Haugland,[1,2] Lennart Schmidt,[1] Ioannis G. Kevrekidis,[2,3] and Katharina Krischer[1,a)]

[1]*Physik-Department, Nonequilibrium Chemical Physics, Technische Universität München, James-Franck-Str. 1, D-85748 Garching, Germany*
[2]*Institute for Advanced Study — Technische Universität München, Lichtenbergstr. 2a, D-85748 Garching, Germany*
[3]*The Department of Chemical and Biological Engineering, Princeton University, Princeton, New Jersey 08544, USA*

(Received 29 February 2016; accepted 13 July 2016; published online 2 August 2016)

We present a universal characterization scheme for chimera states applicable to both numerical and experimental data sets. The scheme is based on two correlation measures that enable a meaningful definition of chimera states as well as their classification into three categories: *stationary*, *turbulent*, and *breathing*. In addition, these categories can be further subdivided according to the time-stationarity of these two measures. We demonstrate that this approach is both consistent with previously recognized chimera states and enables us to classify states as chimeras which have not been categorized as such before. Furthermore, the scheme allows for a qualitative and quantitative comparison of experimental chimeras with chimeras obtained through numerical simulations. *Published by AIP Publishing.* [http://dx.doi.org/10.1063/1.4959804]

The paper "Coexistence of Coherence and Incoherence in Nonlocally Coupled Phase Oscillators" by Kuramoto and Battogtokh published in 2002[1] marks the commencement of intense research activities on a counter-intuitive phenomenon that has come to be known as a chimera state,[2] i.e., the coexistence of coherent and incoherent dynamics in a network of symmetrically coupled identical oscillators. For a long time, the coexistence of coherence and incoherence had been believed to be bound to heterogeneous networks of oscillators, in which oscillators with a similar frequency might mutually synchronize, while those with larger deviations of their frequencies from the mean frequency keep on drifting incoherently. The discovery that an array of identical oscillators, all coupled in an identical way to their neighbors, can also be split into synchronized and drifting groups was likewise surprising as fundamental. The chimera state, being a novel type of dynamic state, can broaden our understanding of transitions from synchrony to "turbulence" and vice versa, and has possible realizations and applications in nature, e.g., in neuroscience[3,4] or hydrodynamics.[5,6] Since the pioneering works in the early years of this millennium, chimera states have been observed in many different systems, ranging from systems with non-local coupling,[7–11] via two-group approximations[12,13] to global all-to-all coupling.[14,15] Due to their robustness to noise, chimera states have also been observed experimentally, e.g., in networks of coupled chemical oscillators,[13] arrays of coupled spatial light modulators,[8] networks of mechanical oscillators,[16] and electrochemical systems.[14] However, the various systems differ strongly in the visual attributes of their dynamic behavior, asking for a systematic categorization. In this paper, we propose a classification scheme based on linear methods, which we believe fulfills the requirements of being universal and simple in its application.

I. INTRODUCTION

Most early studies on chimera states dealt with nonlocally coupled phase oscillators, where coherence refers to phase- and frequency-locked oscillators and incoherence to drifting oscillators, respectively.[1] Lately, more and more chimera patterns were discovered, where coherence and incoherence is of a different nature. One example is a coupled-map chimera, where the individual elements consist of period-two orbits. There, the coexistence pattern is composed of two synchronous regions corresponding to the two realizations of the period-two orbit, with a spatially incoherent interfacial region, where the spatial arrangement of the two states appear in a random and thus incoherent manner.[9] Yet, each state remains a period-2 orbit in time and is thus either synchronized or anti-synchronized to any of the other elements, preserving temporal order. Another example is the so-called amplitude chimera, where the incoherent group is characterized by disorder in the amplitude of the oscillators while all the oscillators in the entire ensemble oscillate with the same frequency.[11] Other coherence/incoherence coexistence patterns differ from the classical chimera state by the variability of coherent and incoherent regions, which might both change their sizes and move in space.[17,18] Furthermore, the stability properties of these diverse chimera states vary greatly. Many chimeras, among them the original one in systems of nonlocally coupled phase oscillators, are transient for a finite number of oscillators, but have a diverging transient time in the continuum limit $N \to \infty$.[19] Others are stable

a)krischer@tum.de

already from small ensemble sizes,[20,21] and still others have finite transient times even in the continuum limit.[11]

These examples illustrate that the original definition of a chimera state as "a spatio-temporal pattern in which a system of identical oscillators is split into coexisting regions of coherent and incoherent oscillators"[22] does not cope with recent developments but calls for a more distinct characterization and refinement. There already exist two approaches towards characterization schemes in minimal networks[20] and for chimeras with non-local coupling,[23] but they are both restricted to a small class of systems.

In this paper, we propose two measures for characterizing chimera states. Although based on linear methods, these quantities provide what we believe to be a clear and simple definition of chimera states, and, furthermore, they allow for an easy distinction between chimera states with different coherence properties and thus provide a useful classification scheme. In addition, our approach is independent of the coupling scheme and the spatial dimension of the system, and not restricted to phase oscillators, such as the (local) Kuramoto order parameter.[1]

The paper is structured as follows: In Section II, we introduce a spatial and a temporal correlation measure applicable to arbitrary data sets and define chimera states with the help of these measures. In Section III, these criteria are applied to experimental and simulated data of different chimera states, and in Section IV, a detailed characterization scheme on the basis of the measures is discussed. Details pertaining to the individual systems and to the numerical methods are given in the supplementary material.[24]

II. CORRELATION MEASURES FOR SPATIAL AND TEMPORAL COHERENCE

A. A measure for correlation in space

For systems with a spatial extent, that is, systems with a local or non-local coupling topology, we employ the local curvature as a measure for the spatial coherence. Hereby, the local curvature of the observable is quantified by the second derivative in one-dimension, or, more generally, by the Laplacian for any number of spatial dimensions. Therefore, we calculate the local curvature at each point in space by re-scaling and applying the discrete Laplacian $\mathbf{D}$ on each snapshot containing the spatial data f. For one snapshot at time t with one spatial dimension, this operation reads

$$\begin{aligned}\hat{\mathbf{D}}f &= \Delta x^2 \mathbf{D}f \\ &= f(x+\Delta x,t) - 2f(x,t) + f(x-\Delta x,t),\end{aligned} \tag{1}$$

where each data point in f can be either real, complex, or of any higher dimension. In order to clarify this concept, consider the chimera state observed by Kuramoto and Battogtokh in a ring of non-locally coupled phase oscillators.[1] One realization of the chimera state is depicted in Figure 1(a). Through the application of the discrete Laplace operator, this snapshot is mapped onto a new function as shown in Figure 1(b), with D_m indicating the maximal value of $|\hat{\mathbf{D}}|$. Note that for phase oscillator systems, we apply this operator on the data in the complex plane, that is the phase oscillators are located on a ring with constant amplitude A. Then, D_m corresponds to the curvature at an oscillator whose two neighbors are shifted 180° in phase, i.e., whose neighboring oscillators are located on opposite positions on the circle. With the re-scaling obtained by multiplying the Laplacian with Δx^2 in Eq. (1), D_m converges to $4A$ in the continuum limit. In the synchronous regime $\lim_{N\to\infty} |\hat{\mathbf{D}}| = 0$. This means that the synchronous regime is projected onto the x-axis through this transformation, while in the incoherent regime $|\hat{\mathbf{D}}|$ is finite and exhibits pronounced fluctuations. Consequently, when we consider the normalized probability density function g of $|\hat{\mathbf{D}}|$, $g(|\hat{\mathbf{D}}| = 0)$ measures the relative size of spatially coherent regions in each temporal realization. For a fully synchronized system $g(|\hat{\mathbf{D}}| = 0) = 1$, while a totally incoherent system gives a value $g(|\hat{\mathbf{D}}| = 0) = 0$. A value between 0 and 1 of $g(|\hat{\mathbf{D}}| = 0)$ indicates coexistence of synchrony and incoherence.

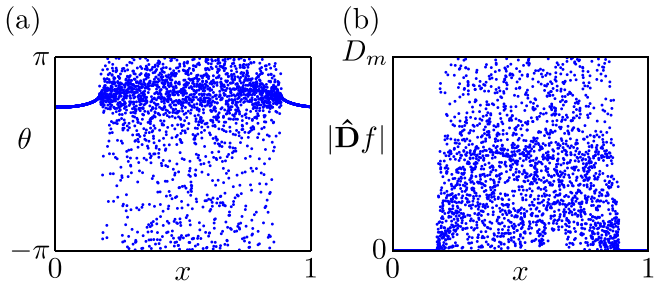

FIG. 1. (a) Snapshot of the Kuramoto model,[1] section I in the supplementary material,[24] after the initial conditions decayed. (b) Absolute value of the local curvature obtained by applying the discrete Laplace operator on the data set shown in (a).

Given this discussion, two important aspects have to be considered. First, the definition of spatial coherence and incoherence is not absolute, but has to be compared to the maximal curvature in each system. Thus, we argue that the characterization of coherence and incoherence is relative and depends on the individual system. Second, even in the coherent region, there might be some minor change in state (cf. Figure 1(a) above) leading to a non-zero curvature. Hence, we are convinced that in order to characterize something as coherent or incoherent, a threshold value is inevitable, although, as will be shown later, the exact position of the threshold does not change the qualitative outcome.

Considering the two arguments above, we propose that for spatially extended systems, a point for which the absolute local curvature is less than one percent of the maximum curvature present in the system should be characterized as coherent, and as incoherent otherwise.

With the threshold $\delta = 0.01 D_m$, our first correlation measure,

$$g_0(t) := \int_0^{\delta} g(t, |\hat{D}|) d|\hat{D}|, \tag{2}$$

can be used to describe the spatial extent occupied by coherent oscillators, even for systems beyond coupled phase oscillators. An example of g for the Kuramoto model is shown in Figure 2(a). Note that, in general, g is time dependent. Figure 2(b) shows $g_0(t)$ as a function of time. The value of $g_0(t)$ of about 0.3 confirms the interpretation of the state as a

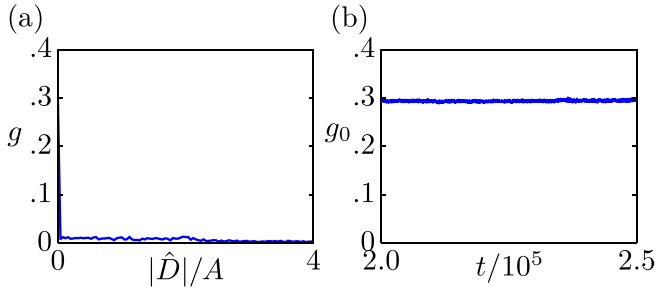

FIG. 2. (a) Probability distribution function g of the discrete Laplace operator applied on the snapshot of Figure 1(a). (b) Temporal evolution of $g_0(t)$ for a longer time series of the Kuramoto model.

chimera state, while its time-independence reveals that the degree of coherence is stationary.

For systems without a spatial dimension, i.e., systems with solely global coupling, curvature is not defined. Nevertheless, we argue that the pairwise Euclidean distances between the values of all oscillators, f_i,

$$\tilde{\mathbf{D}} = \{\tilde{D}_{ij}\} = \|f_i - f_j\|, \quad i \neq j, \tag{3}$$

are a good measure for synchrony/asynchrony. Again, from the normalized probability density function g of $\tilde{\mathbf{D}}$, a variable,

$$\tilde{g}_0(t) := \sqrt{\int_0^{\delta} g(t, |\tilde{D}|) d|\tilde{D}|}, \tag{4}$$

can be obtained that is a measure for the relative amount of correlated oscillators. Here, the square root arises due to the fact that by taking all pairwise distances, the probability of oscillators i and j both being in the synchronous cluster equals $(N_0/N)^2$, with N_0 being the number of the synchronous oscillators. Since both measures, $g_0(t)$ and $\tilde{g}_0(t)$, describe the same property, that is, the degree of spatial synchronization of the system, we only use $g_0(t)$ as notation in the following.

As an illustration, consider the two groups of globally coupled phase oscillators investigated by Abrams *et al.*[12] An exemplary snapshot is depicted in Figure 3(a), where oscillators 1,…, $N/2$ belong to group 1 and oscillators $N/2+1$,…, N constitute group 2. Clearly, group 1 is synchronous while the oscillators in group 2 behave incoherently. In the parameter region considered, a breathing of the chimera as expressed through an oscillation of the variance of the incoherent cluster was reported.[12] The temporal evolution of $g_0(t)$ is shown in Figure 3(b). It can be observed that $g_0(t)$, i.e., the relative

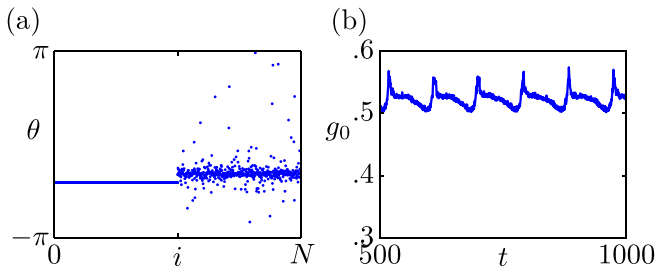

FIG. 3. (a) Snapshot of a realization of the chimera state observed in the two-group model,[12] section II in the supplementary material.[24] (b) Temporal evolution of $g_0(t)$.

amount of partially synchronized oscillators, evolves periodically and "breathes" over time. Therefore, the temporal evolution of $g_0(t)$ allows for the discrimination between chimeras with constant and oscillating partial synchronization. We term these *stationary* and *breathing* chimeras, respectively. The latter term has been adapted from the literature, since the Kuramoto order parameter r exhibits the qualitatively same temporal behavior as g_0.[12] Note that the two approaches above are independent of the spatial dimension and the number of variables of the different systems. This makes $g_0(t)$ a versatile tool for the classification of multifaceted data sets such as those obtained from chimera states.

B. A measure for correlation in time

In addition to the measure for the spatial correlation discussed in Section II A, the temporal correlation of the individual oscillators provides valuable information for a distinction between different chimera dynamics as well. Suppose X_i and X_j are the real or complex time series of two individual oscillators with μ_i, μ_j and σ_i, σ_j their respective means and standard deviations. Then, consider the pairwise correlation coefficients,

$$\rho_{ij} = \frac{\langle (X_i - \mu_i)^* (X_j - \mu_j) \rangle}{\sigma_i \sigma_j}, \tag{5}$$

with $\langle \cdot \rangle$ indicating the temporal mean and $*$ complex conjugation. Note that $\rho_{ij} = 1$ for linearly correlated time series, $\rho_{ij} = -1$ for linearly anti-correlated time series and $|\rho_{ij}| = 1, \angle \rho_{ij} = \alpha$ for complex time series with a constant phase shift of α. That means, the normalized distribution function h of

$$\hat{\mathbf{R}} = \{|\rho_{ij}|\}, \quad i \neq j \tag{6}$$

is a measure for the correlation in time. For static chimera states, where the coherent cluster is localized at the same position over time, $h(|\rho_{ij}| \approx 1)$ is non-zero. In practice, we consider two oscillators as correlated if $|\rho_{ij}| > 0.99 = \gamma$. For example, consider the Kuramoto model mentioned above. Again, we map the system onto the complex plane with arbitrary constant amplitude A for all oscillators. Then, for the chimera state depicted in Figure 4(a), we calculate the correlation matrix $\hat{\mathbf{R}}$ and its probability distribution function h. The first row of $\hat{\mathbf{R}}$, $\{\rho_{0x}\}$, is shown in Figure 4(b). Note that this approach maps the temporally coherent part onto 1, cf. Figure 4(b). The distribution function h is depicted in Figure 5(a). It exhibits a distinct peak at $|\rho| = 1$, indicating that the chimera state is static, i.e., that the majority of oscillators does not change its "group affiliation." We suggest to term this kind of chimera state a *static* chimera. The peak at $|\rho| \approx 0.5$ arises due to the partial linear correlation between oscillators at $x \approx 0.5$ and synchronous oscillators, cf. Figure 4(b). The percentage of the time-correlated oscillators can now be quantified with

$$h_0 := \sqrt{\int_{\gamma}^{1} h(|\rho|) d|\rho|}, \tag{7}$$

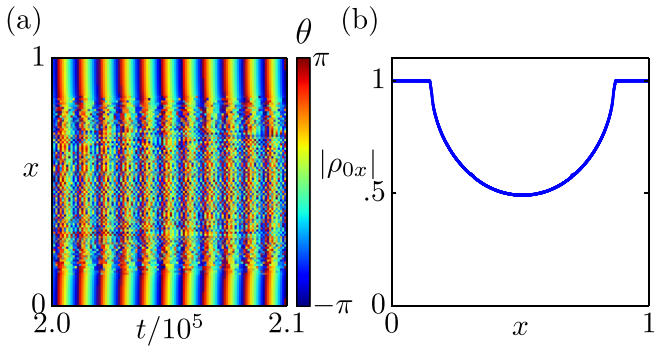

FIG. 4. (a) Temporal evolution of the phase θ in the Kuramoto model,[1] section I in the supplementary material.[24] (b) Pairwise correlation coefficients ρ_{0x} between the oscillator at $x = 0$ and the remaining oscillators.

e.g., $h_0 \approx \sqrt{0.08} \approx 0.28$ for the Kuramoto model, see Figure 5(b).

Note that h_0 does not always reflect the size of the synchronized cluster. This is especially the case when coherent and incoherent regimes are non-static and perform spatial movements over time. Then, h_0 is much smaller than $g_0(t)$ and may vanish for large enough time windows. h_0 coincides with g_0, cf. Figure 5(b), if and only if the chimera is static and no spatial coherence is present in the incoherent cluster.

III. EXAMPLES OF CHIMERA STATES AND THEIR CHARACTERIZATION

As shown in Section II, $g_0(t)$ of the Kuramoto model remains constant in time and, in addition, coincides with h_0. This indicates the constant phase relation between the coherent and incoherent part and their spatial stationarity in time. The same qualitative behavior can be observed in many different non-locally coupled dynamical systems, such as in non-locally coupled Stuart-Landau oscillators investigated by Bordyugov *et al.*[7] and in chimera states observed by Sethia and Sen in a non-locally coupled version of the complex Ginzburg-Landau equation (CGLE).[10] A snapshot and the observables $g_0(t)$ and h_0 of the latter are depicted in Figures 6(a) and 6(b), respectively. If h_0 is larger than 0, independent of the size of the regarded time frame, then one can conclude that the chimera state is stationary in the sense that the incoherent and synchronous patches do not move. According to our definition above, this chimera state is a *static* chimera. Moreover, the finite values of $g_0(t)$ and h_0

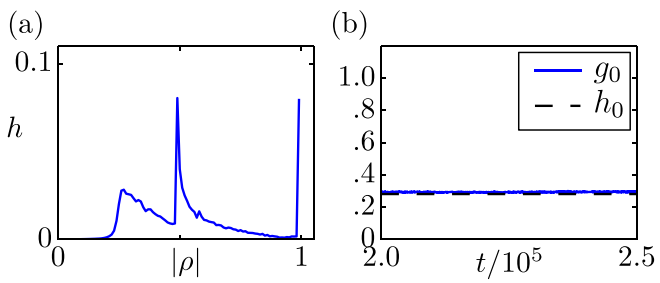

FIG. 5. (a) Distribution function h. (b) Temporal evolution of $g_0(t)$ and the value of h_0, obtained from the same time interval. Note that h_0 is not a function of time and is shown here only for comparison with $g_0(t)$.

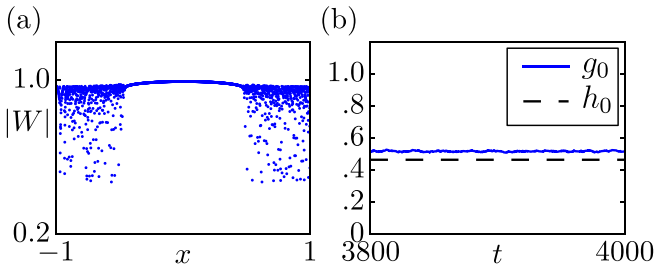

FIG. 6. (a) Snapshot of the amplitude of the amplitude-mediated chimera,[10] section III in the supplementary material.[24] (b) $g_0(t)$ and h_0 of the amplitude-mediated chimera state.

indicate that the desynchronized dynamics are both *spatially* and *temporally* incoherent.

An example of a static chimera state not exhibiting temporal incoherence was examined by Omelchenko *et al* in a system of non-locally coupled maps with a period-2 orbit,[9] and subsequently experimentally realized by Hagerstrom *et al.*[8] As depicted in Figure 7(a), the individual realizations are located on two stable branches. As evident from Figure 7(b), for these chimeras $g_0(t)$ is constant and smaller than 1, while h_0 equals 1. The value of $g_0(t)$ between 0 and 1 affirms that we are dealing with a chimera state, while the fact that $h_0 = 1$ attests to the absence of any temporal incoherence.

As already mentioned in Section II A, the temporal evolution of $g_0(t)$ can be used to identify different dynamic behaviors of chimera states. Apart from being constant, $g_0(t)$ can oscillate in time for a *breathing* chimera state, as already shown in Figure 3(b) for the two-groups approximation.[12] Another example is the so-called type II chimera, which was reported in the CGLE with nonlinear global coupling.[14] The temporal evolution of the absolute value of the complex amplitude and the observables $g_0(t)$ and h_0 are depicted in Figures 8(a) and 8(b), respectively. In Figure 8(b), the oscillatory behavior of $g_0(t)$ is evident, indicating partial synchronization also in the incoherent regime. Note that within the incoherent cluster, there are always homogeneous patches, leading to the offset between $g_0(t)$ and h_0.

Besides oscillating in time, the observable $g_0(t)$ can also vary irregularly. Such a behavior can be observed in the so-called type I chimera in the CGLE with linear global coupling.[18] A representative evolution of the modulus of the complex amplitude W and the corresponding measures $g_0(t)$ and h_0 are depicted in Figures 9(a) and 9(b), respectively. Note that h_0 is significantly larger than 0, indicating that the

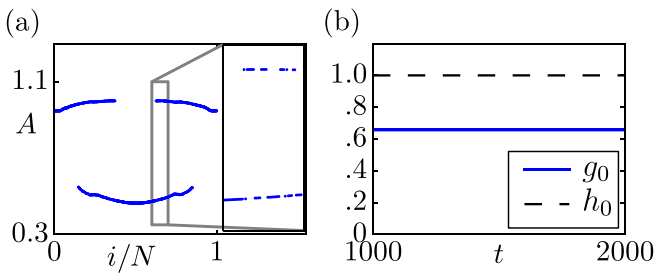

FIG. 7. (a) Snapshot of the chimera state observed by Omelchenko *et al.* (Ref. 9) and Hagerstrom *et al.*,[8] section IV in the supplementary material.[24] In the right part a magnification of the dynamics in the indicated rectangle is shown. (b) $g_0(t)$ and h_0 of the chimera state in (a).

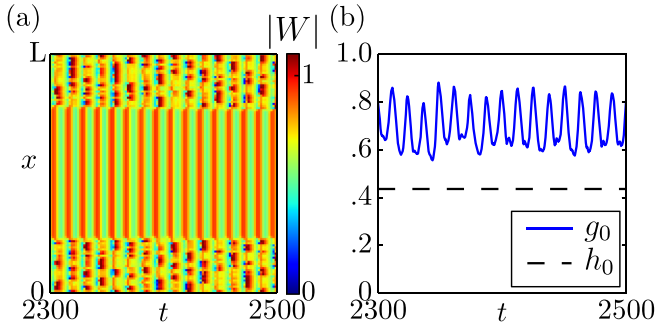

FIG. 8. (a) Temporal evolution of the modulus of a one-dimensional simulation of the type II chimera state observed in the modified CGLE,[14] section VII in the supplementary material,[24] with $L = 1000$. (b) $g_0(t)$ and h_0 calculated from the data shown in (a).

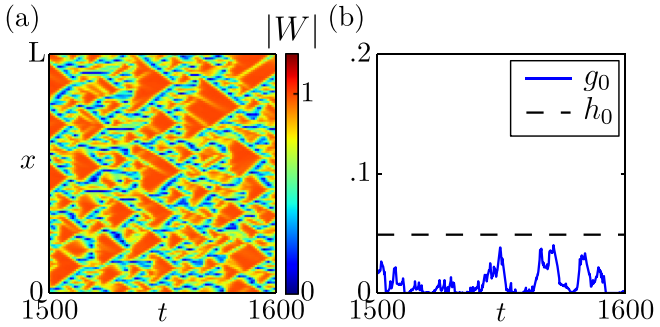

FIG. 10. (a) Temporal evolution of the modulus of the complex amplitude of the one-dimensional CGLE showing spatio-temporal intermittency,[25] section V in the supplementary material.[24] (b) $g_0(t)$ and h_0 calculated from the data shown in (a).

chimera state is static. The irregularity in $g_0(t)$ arises from spatio-temporal intermittency, which appears spontaneously in the turbulent regime, leading to the emergence of patches of oscillators that are synchronous with the coherent region and shrink and disappear with time. Non-stationary chimera states with irregular phase boundaries were also reported by Bordyugov *et al.*,[7] who named this state a *turbulent* chimera. We adapt this expression for general chimera states with irregular variation of the partial synchronization, $g_0(t)$.

Dynamics resembling the type I chimera in some aspects is the spatio-temporal intermittency as observed in the CGLE.[25] A realization of the spatio-temporal intermittency in the one-dimensional CGLE is shown in Figure 10(a). In Figure 10(b), the irregular evolution of $g_0(t)$ is apparent. However, in contrast to the type I chimera discussed above, $g_0(t)$ drops to zero at different points in time. This means that the coherent part, and with it the coexistence between synchrony and incoherence, vanishes completely from time to time. Therefore, spatio-temporal intermittency should not be considered to represent a chimera state. h_0 is also small (<0.05), and results from the correlation of neighboring points due to diffusion.

Dynamics with reversed roles, which are turbulent patches appearing in an otherwise homogeneous regime, are found in the CGLE with linear[17] and non-linear global coupling[18] and are called localized turbulence. An example is shown in Figure 11, with a snapshot of the modulus of a two-dimensional simulation in (a) and the temporal evolution of a one-dimensional cut in (b). The corresponding correlation measures $g_0(t)$ and h_0, calculated from the two-dimensional spatio-temporal data with system size $L = 200$, are depicted in Figure 12(a). The fluctuating value of $g_0(t)$ suggests that the degree of coherence changes with time. A strong increase of the synchronous part occurs at $t \approx 1350$, indicating a strong non-stationarity. However, calculations with larger system sizes suggest that the variations vanish in the thermodynamic limit $N \to \infty$. An illustration is depicted in Figure 12(b), where $g_0(t)$ was calculated from two-dimensional simulations of systems with $L = 2000$.

A characteristic feature of localized turbulence, as compared to all chimera states discussed above, is that the turbulent islands are composed of several incoherent "bubble-like" structures, which move erratically in the spatial domain. Bubbles disappear or pop up through division of existing bubbles. Due to this steady motion of the turbulent islands, the fraction of the coherent time series as measured by h_0 is small, and vanishes if the time window is chosen large enough. The same holds for the alternating chimeras observed by Haugland *et al.*,[26] where the turbulent part alternates with the homogeneous regime in time (not shown).

A. Transient chimeras

So far, we did not consider the long-term stability of the chimera states yet. However, especially in the context of chimera states, defining a stability concept is an important issue.

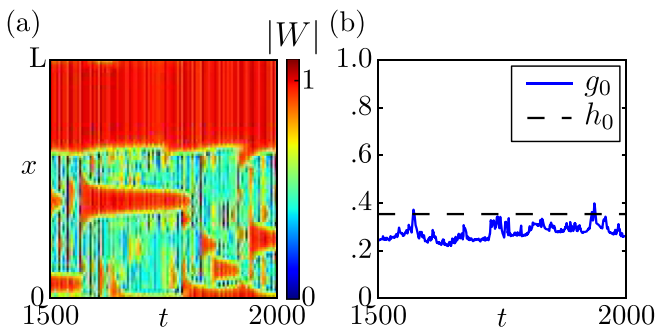

FIG. 9. (a) Temporal evolution of the modulus of the complex amplitude of the type I chimera state observed in the CGLE with linear global coupling,[18] section VI in the supplementary material,[24] with $L = 200$. (b) $g_0(t)$ and h_0 calculated from the data shown in (a).

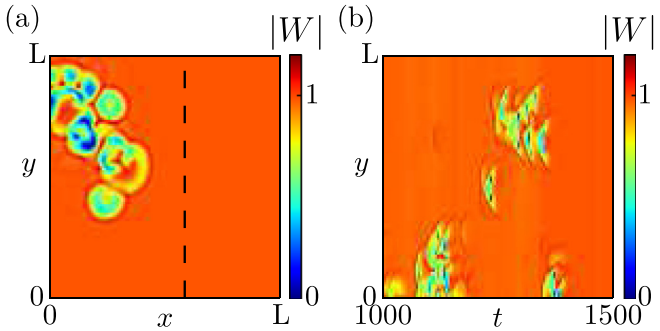

FIG. 11. (a) Snapshot of the amplitude of the localized turbulence[17] at $t = 1500$ with $L = 200$, section VI in the supplementary material.[24] (b) Temporal evolution of a one-dimensional cut at the x-value indicated by the dashed line in (a).

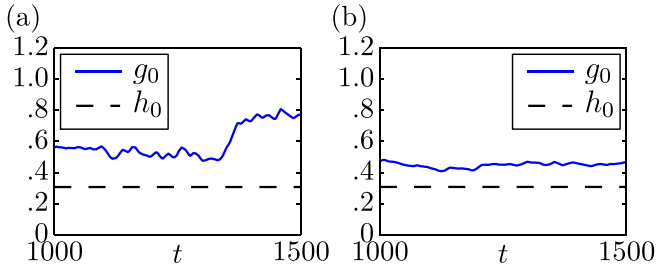

FIG. 12. (a) $g_0(t)$ and h_0 of the localized turbulence with $L = 200$. (b) $g_0(t)$ and h_0 of the localized turbulence with domain length $L = 2000$.

While various chimera states, as the type I and type II chimeras mentioned above, are the only attractors for a specific parameter region, and as such are stable, many other chimera states including those of the Kuramoto model are long-term transients with infinite transient time in the continuum limit $N \to \infty$.[19] Then, there exist states encompassing coexistence of coherence and incoherence that collapse to the homogeneous state after a finite time even for $N \to \infty$. An example thereof is the so-called amplitude chimera.[11] The space-time realization of such a state is depicted in Figure 13(a), Figure 13(b) shows the evolution of $g_0(t)$. Amplitude chimeras resemble the chimeras found in coupled period-2 maps (cf. Figure 7) insofar as they are composed of two coherent domains with anti-phase behavior that are separated by a spatially incoherent interfacial region. In the latter region, the absolute values of the amplitudes vary erratically in space but each oscillator is strictly periodic with a frequency equal to the frequency of the synchronous regions. The spatial incoherence renders $g_0(t)$ smaller than 1. However, as investigated in detail by Loos *et al.*[27] and also evident from Figure 13, the chimera-like dynamics are not stable. A transition to full synchronization can be observed, i.e., $g_0(t) = 1$ after a finite time interval. In this case, the lifetime of the chimera state strongly depends on the choice of the initial conditions and asymptotically approaches a constant value in the continuum limit.[27]

We consider it meaningful to discriminate between transient chimeras and chimera states which are attractive in the continuum limit. Therefore, we suggest to introduce a separate class *transient* chimeras for states with $0 < g_0(t) < 1 \forall t < t_0$ and $g_0(t) = 1 \vee g_0(t) = 0$ at some transient time t_0.

Another remarkable case that created controversy as to its characterization as a chimera was reported by Falcke and

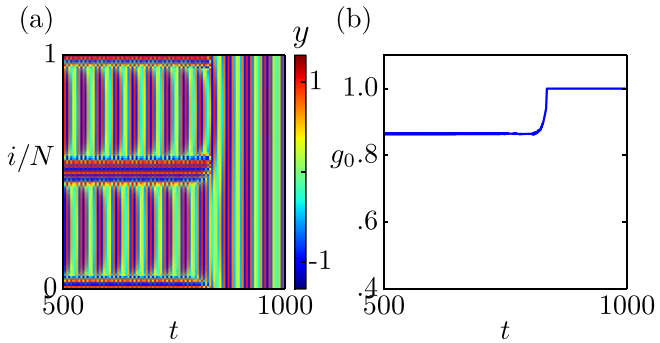

FIG. 13. (a) Temporal evolution of the imaginary part, y, of the so-called amplitude chimera observed by Zakharova *et al.*,[11] section VIII in the supplementary material.[24] (b) $g_0(t)$ of the chimera shown in (a).

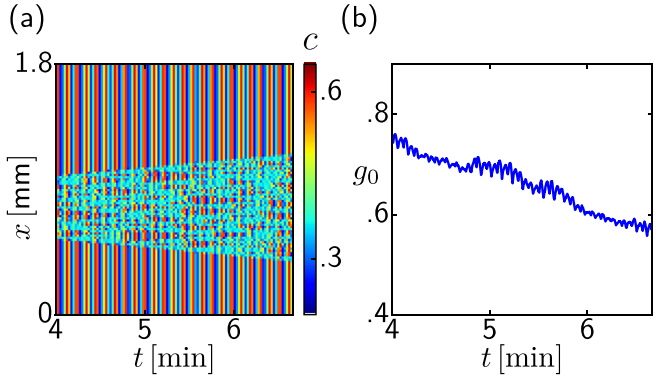

FIG. 14. (a) Temporal evolution of the CO-coverage c, section XI in the supplementary material.[24] (b) $g_0(t)$ of the dynamics shown in (a).

Engel in a globally coupled version of the CO-oxidation model.[28–30] There, turbulent patches appeared in an otherwise homogeneously oscillating background, similar to the localized turbulence discussed above. But, in contrast to the behavior in the localized turbulence, no turbulent bubbles ever disappear. A one-dimensional simulation is depicted in Fig. 14(a), with the corresponding measure $g_0(t)$ plotted in Fig. 14(b). There, the incoherent region expands into the synchronously oscillating domains with an approximately constant velocity that is strongly dependent on the diffusion coefficient D. This non-stationarity manifests itself in the overall systematically declining behavior of $g_0(t)$. In such a case, a longer simulation time is necessary in order to verify that $g_0(t)$ vanishes after a finite time interval, which was confirmed for the present case. Since it mediates a transition from an unstable to a stable state, it fulfills the above defined criteria for a *transient* chimera state. We thus classify it accordingly.

B. Experimental observation of chimeras

Chimeras have also been observed in experimental setups.[8,13,14] In this section, we apply our approach to experimental data as described by Schönleber *et al.*[31] In this system, the thickness of a SiO_2 layer on a Si-electrode oscillates due to simultaneous electrochemical oxidation and etching. Changes in the SiO_2 thickness are measured via ellipsometric imaging. A snapshot of a measurement is depicted in Figure 15(a), with the color indicating the thickness of the oxide layer. The experimental data was processed using a moving

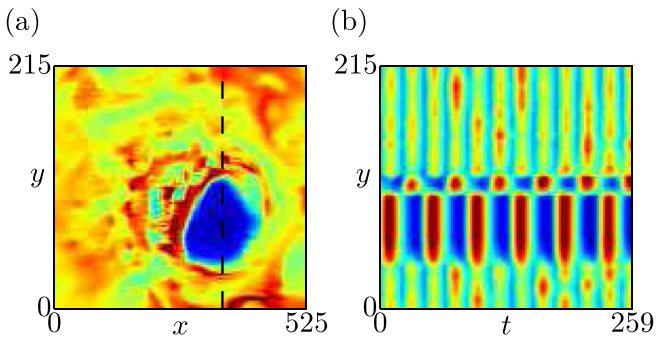

FIG. 15. (a) Snapshot of the SiO_2 thickness on a Si-electrode in pseudocolors. (b) Temporal evolution of a one-dimensional cut as shown in (a).

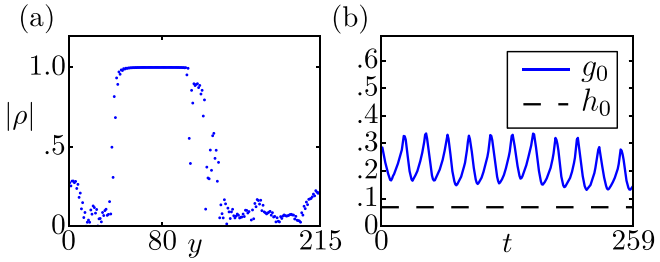

FIG. 16. (a) Correlation coefficients for $y = 80$ for the one-dimensional cut shown in Fig. 15(b). (b) $g_0(t)$ and h_0 for the whole data set.

average over the last 10 time frames. The temporal evolution of a one-dimensional cut is shown in Figure 15(b), where the homogeneous oscillation of a small region in an otherwise inhomogeneously oscillating background can be observed. Figure 16(a) shows the pairwise correlation coefficients of the cross-section with a point inside the coherent cluster (here $y = 80$): a strong linear correlation within this cluster and the diminishing correlation with the remaining oscillators is evident. In Figure 16(b), the behavior of $g_0(t)$ with time and the value of h_0 are shown. They are remarkably similar to type II dynamics as depicted in Figure 8. Hence, we can conclude that the observed experimental chimera is of the *breathing* type. The smallness of h_0 originates from the fact that the coherent cluster is relatively small.

IV. CLASSIFICATION SCHEME

Above, we introduced two correlation measures, $g_0(t)$ and h_0, which allow a quantification of coherence and incoherence in dynamical systems. For phase oscillators, the local Kuramoto order parameter already quantifies the degree of incoherence as a function of space and time. In contrast, our global measure $g_0(t)$ yields information about the total relative sizes of the coherent and incoherent parts of the system, but does not contain information about local properties within the incoherent group. Nevertheless, it exhibits distinct qualitative types of temporal behavior for chimera states with visibly different dynamic features, and thus, like the local order parameter, can be used to discriminate between chimeras, transient chimeras, and other types of dynamics. Its main advantage is its unrestricted applicability, not only to ensembles of phase oscillators but also to any type of dynamical system. Thus, $g_0(t)$ allows for a simple and straightforward classification of general chimera states.

For $g_0(t)$ equal to 0 or 1, one of the two phases, the coherent ($g_0(t) = 0$) or incoherent one ($g_0(t) = 1$), does not exist. This contradicts the requirement of "coexistence," and we argue that dynamical states where this occurs should be differentiated from chimera states. This includes spatio-temporal intermittency, the turbulent patterns in the CO model and the amplitude-chimeras shown in Figure 13. Yet, for the latter two, $0 < g_0(t) < 1$ is valid for a long time interval. Therefore, we suggest that these states are categorized as *transient* chimeras. In the case of intermittency, $g_0(t)$ fluctuates constantly, thereby attaining a value of 0 after arbitrary periods of time. It is therefore differentiated from chimera states.

Chimera states, i.e., states with $0 < g_0(t) < 1$, can then be classified into three groups:

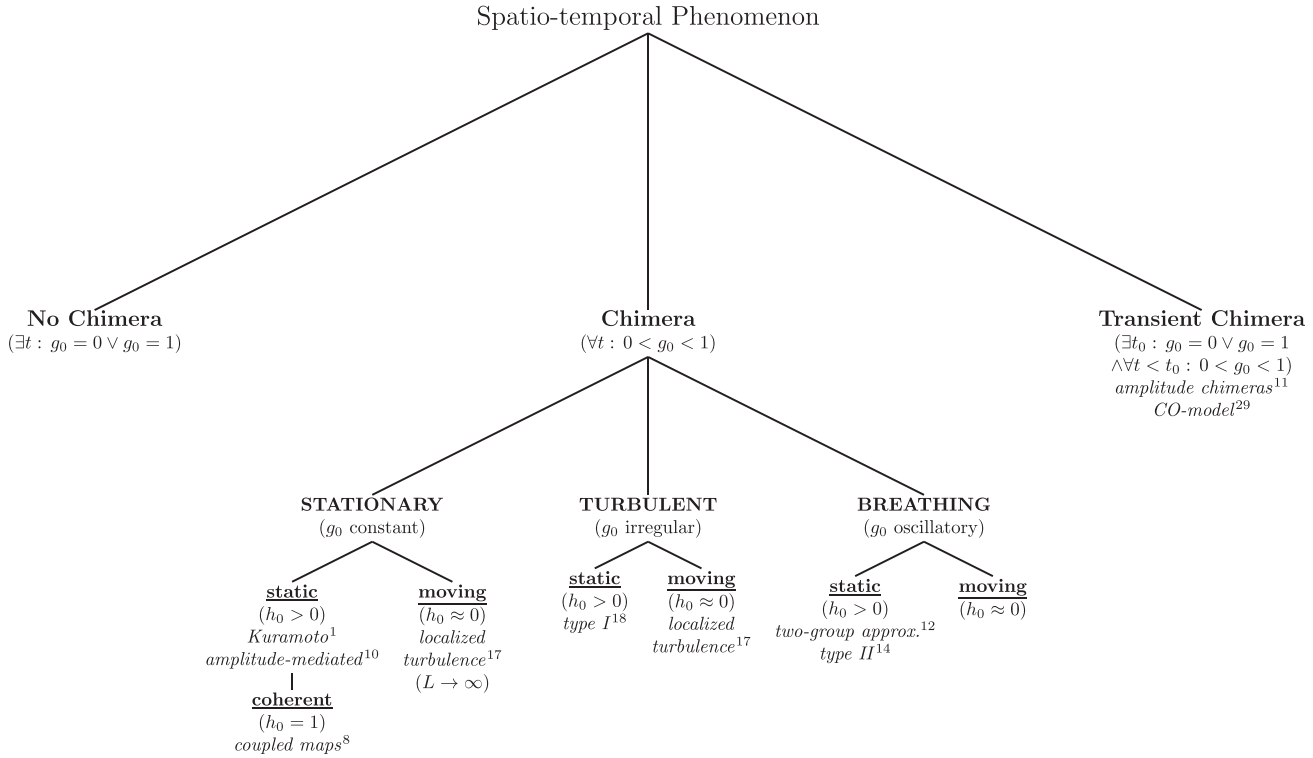

FIG. 17. Characterization of chimera states by means of $g_0(t)$ and h_0. The different examples of chimera states discussed in this paper are given in italics. In order to distinguish between no chimera and transient chimera, the transient time t_0 has to be much larger than the characteristic time of the uncoupled dynamics.

(1) Stationary chimeras: Chimera states with constant coherent cluster size $g_0(t)$
(2) Turbulent chimeras: Chimera states where the temporal evolution of $g_0(t)$ is irregular
(3) Breathing chimeras: States in which the behavior of $g_0(t)$ is periodic.

Note that there might be some ambiguity in the assignment to these sub-categories, since the boundaries between stationary/turbulent and turbulent/oscillatory are rather fluent.

Based on the temporal correlation measure h_0, these groups can be further divided into three subclasses:

(a) *Static chimeras*, in which the coherent cluster is confined to the same position in space over time. That means, h_0 is non-zero and independent of the time window evaluated.
(b) *Moving chimeras*, where h_0 vanishes if the regarded time window is taken sufficiently large.
(c) *Time-coherent chimeras*, that is chimera states with no temporal incoherence and thus $h_0 = 1$.

These criteria are summarized in a chimera classification scheme shown in Figure 17. The examples discussed in Sections II and III are assigned accordingly in the classification tree.

In conclusion, we have introduced two observables, $g_0(t)$ and h_0, that are a measure for the degree of spatial and temporal coherence, respectively, and allow for a discrimination between different types of chimeras from simulated or experimental spatio-temporal data sets. All examples from literature considered here could be assigned to one of the classes. We verified the generality of the approach with additional examples, such as the FitzHugh-Nagumo[32] and Rössler models.[33] Note, however, the scheme does not distinguish between single- and multi-headed chimeras. Furthermore, it is likely that future studies will reveal additional phenomena which the method does not account for at the current stage. However, even in this case, the classification scheme should present a useful base skeleton that can be expanded as new discoveries will dictate.

ACKNOWLEDGMENTS

We thank Maximilian Patzauer and Konrad Schönleber for providing the experimental data and for fruitful discussions. Financial support from the *Institute for Advanced Study - Technische Universität München*, funded by the German Excellence Initiative, and the cluster of excellence *Nanosystems Initiative Munich (NIM)* is gratefully acknowledged.

[1]Y. Kuramoto and D. Battogtokh, "Coexistence of coherence and incoherence in nonlocally coupled phase oscillators," Nonlinear Phenom. Complex Syst. **5**, 380–385 (2002).
[2]D. M. Abrams and S. H. Strogatz, "Chimera states for coupled oscillators," Phys. Rev. Lett. **93**, 174102 (2004).
[3]C. R. Laing and C. C. Chow, "Stationary bumps in networks of spiking neurons," Neural Comput. **13**, 1473–1494 (2001).
[4]N. Rattenborg, C. Amlaner, and S. Lima, "Behavioral, neurophysiological and evolutionary perspectives on unihemispheric sleep," Neurosci. Biobehav. Rev. **24**, 817–842 (2000).
[5]D. Barkley and L. S. Tuckerman, "Computational study of turbulent laminar patterns in Couette flow," Phys. Rev. Lett. **94**, 014502 (2005).
[6]Y. Duguet and P. Schlatter, "Oblique laminar-turbulent interfaces in plane shear flows," Phys. Rev. Lett. **110**, 034502 (2013).
[7]G. Bordyugov, A. Pikovsky, and M. Rosenblum, "Self-emerging and turbulent chimeras in oscillator chains," Phys. Rev. E **82**, 035205 (2010).
[8]A. M. Hagerstrom, T. E. Murphy, R. Roy, P. Hövel, I. Omelchenko, and E. Schöll, "Experimental observation of chimeras in coupled-map lattices," Nat. Phys. **8**, 658–661 (2012).
[9]I. Omelchenko, Y. Maistrenko, P. Hövel, and E. Schöll, "Loss of coherence in dynamical networks: Spatial chaos and chimera states," Phys. Rev. Lett. **106**, 234102 (2011).
[10]G. C. Sethia, A. Sen, and G. L. Johnston, "Amplitude-mediated chimera states," Phys. Rev. E **88**, 042917 (2013).
[11]A. Zakharova, M. Kapeller, and E. Schöll, "Chimera death: Symmetry breaking in dynamical networks," Phys. Rev. Lett. **112**, 154101 (2014).
[12]D. M. Abrams, R. Mirollo, S. H. Strogatz, and D. A. Wiley, "Solvable model for chimera states of coupled oscillators," Phys. Rev. Lett. **101**, 084103 (2008).
[13]M. R. Tinsley, S. Nkomo, and K. Showalter, "Chimera and phase-cluster states in populations of coupled chemical oscillators," Nat. Phys. **8**, 662–665 (2012).
[14]L. Schmidt, K. Schönleber, K. Krischer, and V. García-Morales, "Coexistence of synchrony and incoherence in oscillatory media under nonlinear global coupling," Chaos **24**, 013102 (2014).
[15]A. Yeldesbay, A. Pikovsky, and M. Rosenblum, "Chimera like states in an ensemble of globally coupled oscillators," Phys. Rev. Lett. **112**, 144103 (2014).
[16]E. A. Martens, S. Thutupalli, A. Fourrière, and O. Hallatschek, "Chimera states in mechanical oscillator networks," Proc. Natl. Acad. Sci. U.S.A. **110**, 10563–10567 (2013).
[17]D. Battogtokh, A. Preusser, and A. Mikhailov, "Controlling turbulence in the complex Ginzburg-Landau equation II. Two-dimensional systems," Phys. D **106**, 327–362 (1997).
[18]L. Schmidt and K. Krischer, "Chimeras in globally coupled oscillatory systems: From ensembles of oscillators to spatially continuous media," Chaos **25**, 064401 (2015).
[19]M. Wolfrum and O. E. Omel'chenko, "Chimera states are chaotic transients," Phys. Rev. E **84**, 015201 (2011).
[20]P. Ashwin and O. Burylko, "Weak chimeras in minimal networks of coupled phase oscillators," Chaos **25**, 013106 (2015).
[21]L. Schmidt and K. Krischer, "Clustering as a prerequisite for chimera states in globally coupled systems," Phys. Rev. Lett. **114**, 034101 (2015).
[22]M. J. Panaggio and D. M. Abrams, "Chimera states: Coexistence of coherence and incoherence in networks of coupled oscillators," Nonlinearity **28**, R67–R87 (2015).
[23]R. Gopal, V. K. Chandrasekar, A. Venkatesan, and M. Lakshmanan, "Observation and characterization of chimera states in coupled dynamical systems with nonlocal coupling," Phys. Rev. E **89**, 052914 (2014).
[24]See supplementary material at http://dx.doi.org/10.1063/1.4959804 for details on the individual systems and on the numerical methods used.
[25]B. Shraiman, A. Pumir, W. van Saarloos, P. Hohenberg, H. Chaté, and M. Holen, "Spatiotemporal chaos in the one-dimensional complex Ginzburg-Landau equation," Phys. D **57**, 241–248 (1992).
[26]S. W. Haugland, L. Schmidt, and K. Krischer, "Self-organized alternating chimera states in oscillatory media," Sci. Rep. **5**, 9883 (2015).
[27]S. A. M. Loos, J. C. Claussen, E. Schöll, and A. Zakharova, "Chimera patterns under the impact of noise," Phys. Rev. E **93**, 012209 (2016).
[28]M. Falcke and H. Engel, "Influence of global coupling through the gas phase on the dynamics of CO oxidation on Pt(110)," Phys. Rev. E **50**, 1353–1359 (1994).
[29]M. Falcke and H. Engel, "Pattern formation during the CO oxidation on Pt(110) surfaces under global coupling," J. Chem. Phys. **101**, 6255–6263 (1994).
[30]M. Falcke, *Strukturbildung in Reaktions- Diffusionssystemen und globale Kopplung* (Wissenschaft und Technik Verlag Gross, Berlin, Sebastianstr. 84, 1995).
[31]K. Schönleber, C. Zensen, A. Heinrich, and K. Krischer, "Pattern formation during the oscillatory photoelectrodissolution of n-type silicon: Turbulence, clusters and chimeras," New J. Phys. **16**, 063024 (2014).
[32]I. Omelchenko, O. E. Omel'chenko, P. Hövel, and E. Schöll, "When nonlocal coupling between oscillators becomes stronger: Patched synchrony or multichimera states," Phys. Rev. Lett. **110**, 224101 (2013).
[33]I. Omelchenko, B. Riemenschneider, P. Hövel, Y. Maistrenko, and E. Schöll, "Transition from spatial coherence to incoherence in coupled chaotic systems," Phys. Rev. E **85**, 026212 (2012).